**The crystal structure of *Mycobacterium thermoresistibile* MurE ligase reveals the binding mode of the substrate m-diaminopimelate.**

**Nicolas de Oliveira Rossini[a], Catharina dos Santos Silva[a], Marcio Vinicius Bertacine Dias[a,b].**

[a] - Department of Microbiology, Institute of Biomedical Science, University of São Paulo. Av. Prof Lineu Prestes, 1374, CEP 05508-000, São Paulo, SP. Brazil

[b] - Department of Chemistry. The University of Warwick, Coventry, CV4 7AL, UK.

Corresponding author: mvbdias@usp.br and marcio.dias@warwick.ac.uk

**Synopsis**

Structural characterization of *Mycobacterium thermoresistibile* MurE at 1.45Å resolution in complex with ADP and m-DAP shows novel conformational changes when compared to other MurE structures in complex with different ligands.

**Abstract**

The cytoplasmatic biosynthesis of the stem peptide from the peptidoglycan in bacteria involves six steps, which have the role of three ATP-dependent Mur ligases that incorporate three consecutive amino acids to a substrate precursor. MurE is the last Mur ligase to incorporate a free amino acid. Although the structure of MurE from *Mycobacterium tuberculosis* (MtbMurE) was determined at 3.0Å, the binding mode of (meso-Diaminopimelate) m-DAP and the effect of substrate absence is unknown. Herein, we show the structure of MurE from *M. thermoresistibile* (MthMurE) in complex with ADP and m-DAP at 1.4 Å resolution. The analysis of the structure indicates key conformational changes that the substrate UDP-Mur*N*Ac-L-Ala-D-Glu (UAG) and the free amino acid m-DAP cause on the MthMurE conformation. We observed several movements of domains or loop regions that displace their position in order to perform enzymatic catalysis. Since MthMurE has a high similarity to MtbMurE, this enzyme could also guide strategies for structure-based antimicrobial discovery to fight against tuberculosis or other mycobacterial infections.

**Keywords:** murE ligase; peptidoglycan; mycobacteria; bacterial cell wall; enzyme

## 1. Introduction

The peptidoglycan plays a pivotal role in the survival of most bacteria, including actinomycetes, defining the bacterial shape and protecting against lysis by osmotic strength (Egan et al., 2020; Shaku et al., 2020). This structure is constituted by layers of glycans, particularly *N*-acetylglucosamine (Glc*N*ac) and *N*-acetylmuramic acid (Mur*N*ac) linked through a β(1→4) configuration (Vollmer et al., 2008). The layers are further linked through a peptide moiety, which is cytoplasmically synthesized and exported toward the extracellular space coupled to a $C_{55}$ undecaprenyl-phosphate molecule (lipid I) and further glycosaminylated (lipid II) (Egan et al., 2020). This molecule usually is translocated out of the cell membrane by a lipid II flippase (MurJ) (Ruiz, 2016), and in the extracellular space, it is incorporated into the glycan chains by transglycosylases. The pentapeptide is also further cross-linked by DD-transpeptidase and LD-transpeptidases to produce the known rigid structure of the peptidoglycan (Aliashkevich and Cava, 2021; Egan et al., 2015; Libreros-Zúniga et al., 2019; Straume et al., 2021).

As peptidoglycan is a crucial structure for most bacteria, is not surprising that the enzymes responsible for its biosynthesis are the target of several antimicrobials, including β-lactam antibiotics that inhibit transpeptidation reactions (Cochrane and Lohans, 2020), and fosfomycin, which is a validated antibiotic for the inhibition of the first step of cytoplasmatic stem peptide biosynthesis, catalyzed by the enzyme MurA (Hrast et al., 2014; Marquardt et al., 1994). Furthermore, D-cycloserine also targets the enzyme MurF or D-Ala-D-Ala ligase, which incorporates the last two amino acids into the cytoplasmatic stem peptide (Batson et al., 2017).

Usually, the cytoplasmatic biosynthesis of stem peptide moiety of peptidoglycan involves six steps, which are catalyzed by the essential enzymes denominated Mur A to F producing a pentapeptide constituted of L-alanine, D-glutamate, L-Lysine or m-DAP, D-Alanine-D-Alanine, which is further linked to a UDP-Mur*N*ac molecule. The biosynthesis of this stem peptide starts with the enzyme MurA, which incorporates enol pyruvate moiety to the UDP-Glc*N*ac, which is further reduced by MurB to produce UDP-*N*-acetylmuramic acid (UDP-Mur*N*ac). Three amino acids, L-Ala, D-Glu, m-DAP (or L-Lysine) are incorporated into UDP-Mur*N*ac by a series of ATP-dependent Mur ligases, MurC, MurD, and MurE, respectively (Egan et al., 2020). These enzymes are sequentially and structurally related and share similar catalytic mechanisms (Kouidmi et al., 2014;

Smith, 2006). Finally, MurF, also an ATP-dependent enzyme, adds the D-Ala-D-Ala moiety to produce the UDP-Mur*N*ac-pentapeptide precursor (Duncan et al., 1990; Falk et al., 1996). In some bacteria, including mycobacteria, these enzymes have a single gene copy and they are essential for survival (Barreteau et al., 2008; Shinde et al., 2021). Consequently, they are key targets for the development of novel antimicrobials since they are not conserved in eukaryotes. Among these enzymes, one of the most intriguing is MurE, which adds the third amino acid to the UDP-Mur*N*ac-pentapeptide precursor (Kouidmi et al., 2014; Ruane et al., 2013). This enzyme is usually highly selective, with a few exceptions, and discriminates between L-Lysine or m-DAP in Gram-positive and Gram-negative or actinomycetes, respectively (Ruane et al., 2013). The substitution of *Escherichia coli* (Gram-negative) with *murE* from *Staphylococcus aureus* (Gram-positive) results in highly attenuated cells, which promptly undergo lysis (Mengin-Lecreulx et al., 1999). Because of its importance, MurE has been a target of several studies aiming to identify novel lead compounds, particularly in *M. tuberculosis* or in other mycobacteria (Guzman et al., 2015; Hervin et al., 2020; Kouidmi et al., 2014; Zaveri and Kiranmayi, 2016), which also have an m-DAP incorporated into its stem peptide (Alderwick et al., 2015). The development of new antimicrobials against this group of bacteria is very urgent because usually they are of difficult treatment, added to the resistance of most used antimicrobials. Tuberculosis, for example, is worldwide overspread with high mortality and is one of the major causes of death by infectious disease, mostly in countries in Africa, Asia and Latin America (Dean et al., 2022; World Health Organization, 2021).

The structure of *M. tuberculosis* MurE (MtbMurE) was determined at 3.0 Å resolution in the presence of ADP and the substrate UDP-Mur*N*ac-L-Ala-D-Glu (UAG) (Basavannacharya et al., 2010a), which revealed a folding similar to the other bacteria, including MurE and MurD from *E. coli* (Bertrand et al., 1997; Gordon et al., 2001). MurE has three domains, which are responsible for the binding of the different ligands: the N-terminal domain has a Rossmann-like folding and binds the substrate UAG; the central or nucleotide-binding domain has a nucleotide-binding folding and binds the ATP and; the C-terminal domain, which also has a Rossmann-like folding and binds the L-lysine or m-DAP (Gordon et al., 2001; Smith, 2006). The ATP-dependent Mur ligases are known to be very mobile enzymes to provide the correct substrate orientation, particularly for the phosphorylation of L-Lysine or m-DAP carboxylate moiety using ATP, which is

further attacked by the amino group of UAG to produce UDP-Mur*N*Ac-L-Ala-D-Glu-m-DAP (UMT, UDP-Mur*N*Ac-tripeptide) and inorganic phosphate (Kouidmi et al., 2014). So far, most of the structures solved for MurE consist of the complex with UAG substrate (Basavannacharya et al., 2010b) or UMT product (Gordon et al., 2001; Ruane et al., 2013) or ADP (Favini-Stabile et al., 2013). Only recently, the structure of a MurE in its apo form was reported (Jung et al., 2021). To our knowledge, there is no structure of any MurE in the presence of the free amino acid L-Lys or m-DAP and consequently, the conformational changes triggered by the binding of this substrate are unknown.

In order to contribute to the understanding of MurE motions in the presence of different ligands and also to obtain a model with a higher resolution for mycobacteria that could be used in the development of new specific antimicrobials, we have solved the structure of *M. thermoresistibile* MurE (MthMurE) in the presence of ADP and the substrate m-DAP at a resolution of 1.45Å resolution. Our structure shows key conformational changes in loops and domains which are caused by the absence of UAG substrate in comparison to MtbMurE. Also, we could observe the impact of m-DAP itself on the protein conformation, in which our structure is the first one to be obtained with the free form of the amino acid to be incorporated into the UAG substrate.

## 2. Materials and Methods

### 2.1. Protein expression and purification.

A synthetic gene for expression of *M. thermoresistibile* MurE (MthMurE) was obtained commercially from Twist Bioscience and cloned into a pET28a plasmid to produce an N-terminal his-tag. This plasmid was inserted into *E. coli* C41 (DE3) competent cells by heat shock transformation. The cells were grown in LB media and the protein expression was performed by adding 1 mM IPTG to the cultures when the $OD_{600}$ reached 0.6-0.8. The culture was maintained for a further 18 h at 20 °C, 200 rpm, and harvested by centrifugation.

For protein purification, the cells were lysed by sonication using 40 mL of resuspension buffer A (0.2 M NaCl/ 0.01 M $MgCl_2$/ 0.05 M Tris-HCl pH 8.5/ 10% glycerol/) and by adding 2 µM PMSF, 50 µg/ml DNAase and 50 µg/ml lysozyme. The lysate was centrifuged at 35500 *g* at 4°C. The supernatant was loaded into a nickel-filled HisTrap Column connected to an Äkta Start (GE Healthcare Life Sciences) and the protein was eluted using an imidazole gradient from 0 to 600 mM. The fractions containing the protein

of interest were separated, concentrated up to 2 mL and used for an additional purification step of size exclusion chromatography using buffer A and a HiLoad™ 16/600 Superdex™ 200pg column. The presence of protein and its quality were monitored by SDS-PAGE. Peak fractions containing the protein were harvested and concentrated up to 46.5 mg/mL and stored at -80°C until use.

### 2.2. Crystallization and structure determination of MthMurE

MthMurE at 46.5 mg/mL was used for the co-crystallization experiments with ADP and m-DAP. MthMurE was crystallized using the vapor diffusion method by the hanging drop technique. For that, MthMurE was incubated with 24 mM of ADP and 24 mM of m-DAP for 30 minutes on ice, and drops were performed in a siliconized coverslip. Drops of 1:1, 1:2 and 2:1 ratio of reservoir solution and protein solution were prepared. The used crystallization condition was similar to that used for MtbMurE (0.35M $MgCl_2$, 0.1 M Tris, pH 8.5 and 24%-45% PEG 8000) (Basavannacharya et al., 2010b). Large prismatic crystals appeared after 15 days in plates incubated at 18 °C.

Data collection was performed at MANACÁ beamline, SIRIUS, CNPEM, Campinas, Brazil. The X-ray diffraction data were processed using XDS (Kabsch, 2010) and scaled by AIMLESS (Evans and Murshudov, 2013). The molecular replacement was performed by MolRep (Vagin and Teplyakov, 2010) and the structure of *M. tuberculosis* MurE (MtbMurE) in complex with the substrate UDP-Mur*N*AC- dipeptide (UAG) (PDB entry 2XJA) (Basavannacharya et al., 2010a) was used as a probe. The structural refinement was performed by phenix.refine (Liebschner et al., 2019) implemented in the Phenix suite (Adams et al., 2011). The visual inspection, as well as the real space refinement, were assessed using Coot (Emsley et al., 2010). The stereochemistry quality was evaluated using MolProbity (Davis et al., 2007) and the final figures were prepared using PyMOL (Schrödinger, LLC, 2015).

### 2.3.Molecular Dynamics

The protein coordinates were obtained from the MthMurE structure reported in this work. The water and ligand molecules besides ADP were deleted and the Charmm36 force field compatible file was generated using CHARMM-GUI interface. The ADP topology was created using CGenFF server. The forcefield used was Charmm36 (Soteras Gutiérrez et al., 2016) and water models were TIP3P (Madura et al., 1983). The system was solvated

using a dodecahedral solvation-box and the charge balancing for the system was performed by replacing solvent molecules with sodium ions. Energy minimization of the system was performed using GROMACS (Abraham et al., 2015) and the temperature and pressure of the system were equilibrated before the unrestrained molecular dynamics simulation. A 100 ns molecular dynamics was performed using GROMACS and results were analyzed also using GROMACS built-in tools.

## 3. Results and Discussion

### 3.1.The overall structure of MthMurE

Tetragonal MthMurE crystals diffracted up to 1.45Å and the structure in complex with ADP and m-DAP was solved by molecular replacement using the structure of MtbMurE (Basavannacharya et al., 2010a). MthMurE crystals have a single protomer in the asymmetric unit (data not shown). The crystallization conditions are shown in Table 1, the statistics for the X-ray diffraction data processing are also shown in Table 2 and structure refinement is shown in Table 3.

**Table 1** - Crystallization

| | |
|---|---|
| Method | Hanging Drop |
| Plate type | 24 wells Linbro-style plate |
| Temperature (K) | 298.15 |
| Protein concentration | 46.5mg/mL |
| Buffer composition of protein solution | 0.2M NaCl, 0.01M $MgCl_2$, 0.05M TRIS-HCL pH 8.5, 10% Glycerol |
| Composition of reservoir solution | 0.35M $MgCl_2$, 0.1M TRIS, pH 8.5 and 24-45% PEG8000 |
| Volume and ratio of drop | 2µL / 1:1 |
| Volume of reservoir | 500µL |

**Table 2** – Data collection and processing

| | |
|---|---|
| Diffraction source | MANACÁ beamline, SIRIUS, CNPEM, Campinas, Brazil |
| Wavelength (Å) | 0.9772 |
| Temperature (K) | 100 |

| | |
|---|---|
| Detector | DECTRIS PILATUS 2M |
| Space group | $P4_32_12$ |
| *a*, *b*, *c* (Å) | 62.79, 62.79, 238.27 |
| α, β, γ (°) | 90, 90, 90 |
| Resolution range (Å) | 44.4 – 1.45 (1.50 - 1.45) |
| Total No. of reflections | 2193452 (194844) |
| No. of unique reflections | 85464 (8190) |
| Completeness (%) | 100 (97) |
| Redundancy | 25.7 (23.8) |
| $\langle I/\sigma(I)\rangle$ | 21 (1.79) |
| CC1/2 | 1 (0.697) |
| $R_{p.i.m.}$ | 0.024 (0.438) |
| Overall *B* factor from Wilson plot (Å$^2$) | 15.64 |

**Table 3** – Structure solution and refinement

| | |
|---|---|
| Resolution range (Å) | 44.4 – 1.45 (1.50 – 1.45) |
| Completeness (%) | 99.66 (97.40) |
| σ cutoff | 1.350 |
| No. of reflections, working set | 85461 (8190) |
| No. of reflections, test set | 4275 (437) |
| Final $R_{cryst}$ | 0.170 (0.264) |
| Final $R_{free}$ | 0.190 (0.285) |
| No. of non-H atoms | 4510 |
| Protein | 3822 |
| Ligand | 102 |
| Water | 622 |
| R.m.s. deviations | |
| Bonds (Å) | 0.006 |
| Angles (°) | 0.91 |
| Average *B* factors (Å$^2$) | 20.69 |

| | |
|---|---|
| Protein | 18.75 |
| Average Ligands | 23.92 |
| ATP | 33.4 |
| m-DAP | 19.9 |
| Solvent | 32.87 |
| Ramachandran plot | |
| Most favoured (%) | 98 |
| Allowed (%) | 1.19 |
| Molprobity Score | 1.21 |

We modeled the structure from residue 1 to 506, with no gaps in the amino acid chain. This is so far the highest resolution for any reported MurE ligase. MthMurE has, as expected, a similar fold to other Mur enzymes, including MurC, MurD and MurE, from different bacteria, which are constituted by the three globular domains (Zoeiby et al., 2003): The N-terminal domain (2-112), which has a folding similar to a transferrin fragment (Lawrence et al., 1999) and is responsible for the binding of the UDP moiety from UDP-MurNac-peptide substrate; The nucleotide-binding domain (113-353), which has the binding sites for the peptide moiety of UAG and ATP and is the central part of the protein and has a mononucleotide binding folding, commonly found in other ATP binding proteins (Walker et al., 1982); and finally, the Rossman folding C-terminal domain (354-506), which contains the m-DAP binding site (Figure 1).

**Figure 1 - MthMurE structure**

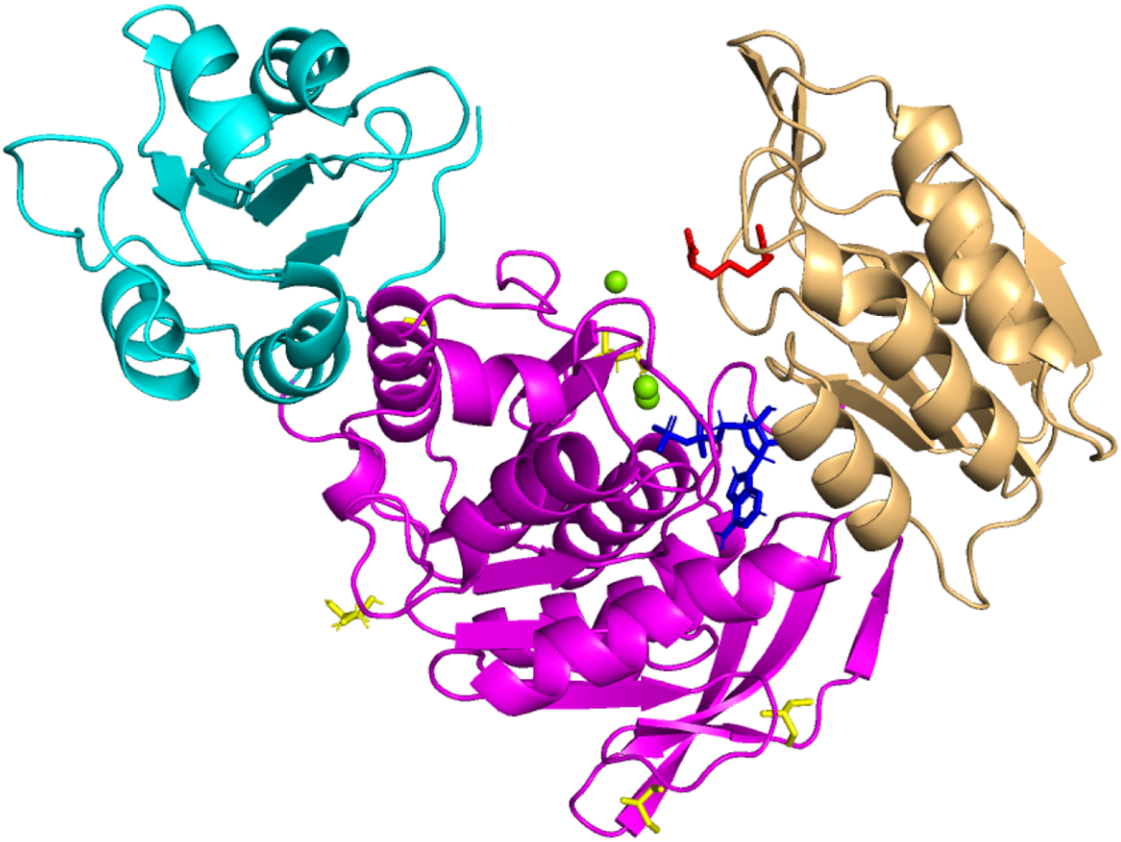

**Fig 1. MthMurE structure**. The N-terminal domain is shown in cyan and is responsible for UAG binding (not shown in the figure). The central or nucleotide-binding domain is in purple and it is responsible for binding the other extremity of the UAG molecule, as well as the ATP molecule (part of ATP is shown as dark blue sticks). The C-terminal domain is in light orange and is responsible for m-DAP binding (m-DAP is shown in red sticks). Glycerol molecules observed in our structure are shown in yellow, while the $Mg^{2+}$ ions are shown as green spheres**.**

The amino acid sequence of MthMurE shares 67% identity with MtbMurE (Supplementary Figure 1). However the structure superposition of these two proteins rendered an rmsd of 1.4Å (Supplementary Figure 2) suggesting that, despite the sequence conservation, these structures, which have been obtained in complex with different ligands, have a moderate level of divergence. The most divergent region is located in the N-terminal, which has an rsmd of 1.3Å, while the C-terminal domains and the nucleotide-binding domain are more similar, with an rmsd of 0.7Å and 0.9Å, respectively. There are three $Mg^{2+}$ ions bond in the structure. These ions are located in the central domain and two of them (we have named them $Mg^{2+}$-1 and $Mg^{2+}$-2 ) seem to be crucial for MurE activity and they perform key interactions with MthMurE, such as Kcx235 (carbamylated

Lys235) for $Mg^{2+}$ -2 (Figure 3F) or to the diphosphate moiety of ADP for $Mg^{2+}$-1 (Figure 2A). The third ion is placed far from the catalytic cavity and probably is an artifact caused by the high $Mg^{2+}$ concentration in the crystallization solution.

### 3.2. ATP binding site

The MthMurE ATP binding site is located at a cavity formed by Thr127, Ser128, Gly129, Lys130, Thr131, Thr132, Glu193 Asn216, Phe316, Asn320 Arg350, Asp365, Ala367 Tyr366, Ala372, Ala375, Val376. The main residues that interact with the adenine moiety are Gly129 and Asn320 (Figure 2A). On the other hand, the main residues that interact with the ribose are Asp365 and Ala367 and, the diphosphate moiety interacts with Thr127, Gly129, Lys130, Thr131, Thr132, Glu193, Ar350 and with the $Mg^{2+}$-1 (Figure 2A). In an overall comparison to MtbMurE, we did not observe any large conformational differences in this region. As mentioned previously most residues are conserved between MthMurE and MtbMurE, except the residues Ala375 (Ser402 in Mtb) and Phe316 (Tyr343 in Mtb) (Supplementary Figures 1 and 2). By the superposition of MthMurE and MtbMurE, it is also possible to observe that the binding of ADP adenine moiety has a similar position in both structures, in contrast to the ribose which has a slightly different conformation (Figure 2B). This could be caused by the effect of the low resolution of the MtbMurE structure or even because of the absence of UAG in our structure, increasing the flexibility of this ADP moiety.

**Figure 2 - Analysis of conformational differences in ADP cavity comparing Mth and Mtb MurE structures.**

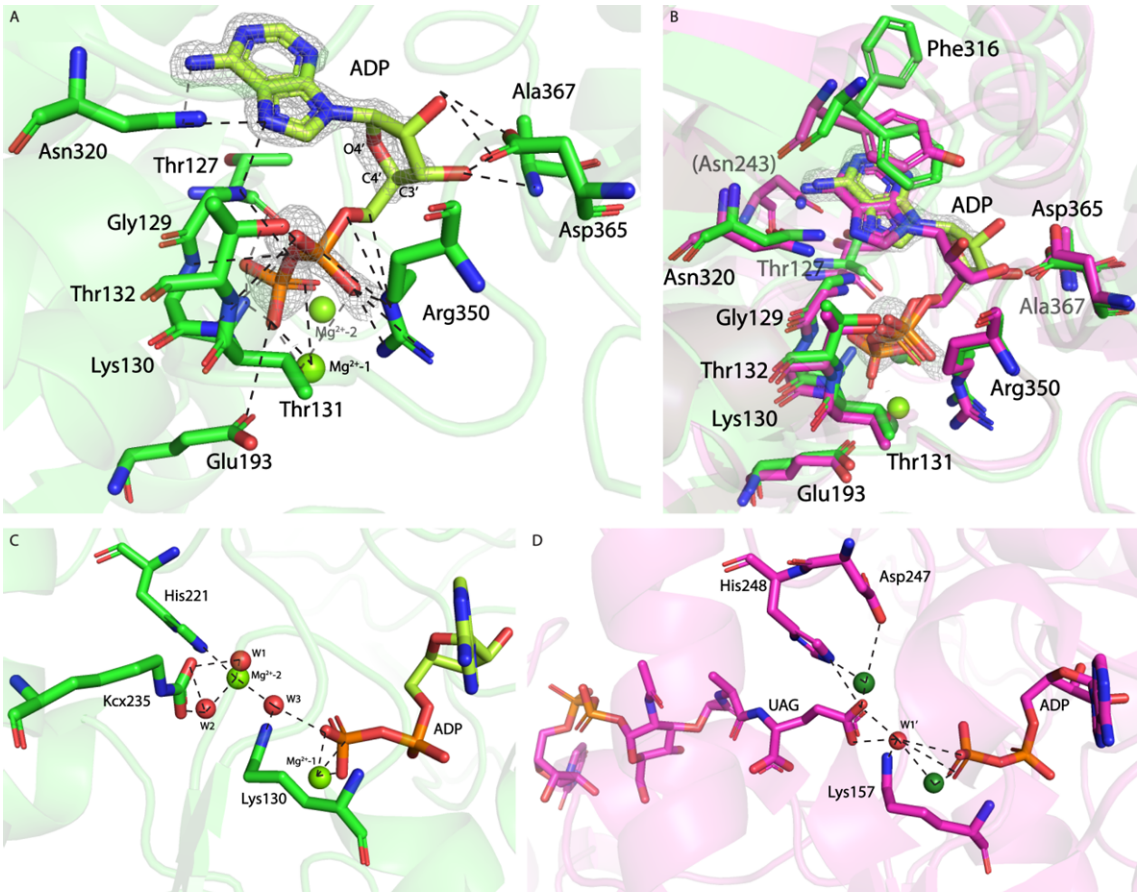


**Fig 2. Analysis of the conformational differences in ADP active site comparing Mth and Mtb MurE structures**. **A –** The MthMurE structure is shown in green. Key residues interacting with ADP are shown in green carbon atoms, in blue are nitrogens and in red oxygens. The carbon atoms from ADP are colored light green. Interactions are represented with dotted black lines. The electron density contours (2Fo-Fc map) for ADP are shown in grey around it at 0.7 sigma / **B** - Superposition of MthMurE and MtbMurE showing the differences in the ADP binding site. The structural $Mg^{2+}$ ion is shown in light green in the MthMurE structure and dark green for MtbMurE./ **C –** Binding network for the ADP binding site in MthMurE. Interactions are shown as black dotted lines. Water molecules are shown as red spheres and $Mg^{2+}$ ions are shown as light green spheres. / **D –** Binding network for the ADP binding site in MtbMurE. $Mg^{2+}$ ions are shown as dark green spheres. PDB entry for MtbMurE structure 2XJA (Basavannacharya et al., 2010a)

Interestingly, the electron density contours for the diphosphate moiety of ADP were weaker than expected, indicating flexibility. To support this hypothesis, we performed a molecular dynamics simulation with a trajectory of 100 ns. By analysis of this data, the ADP molecule showed an average RMSD of about 1.6 Å when compared to the protein backbone, and the most flexible atoms were from the ribose moiety, particularly the oxygen 4' and carbons C3' and C4'. This last one is closely involved in the connection to the diphosphate moiety through carbon C5' (Supplementary Figure 6). These results

contribute to explaining why the diphosphate moiety has more diffuse electron density contours in MthMurE. Comparing the interactions of the ADP binding site of MthMurE and MtbMurE, we also observe that two interactions are not conserved in MthMurE (Figure 2B). The phenyl hydroxy group of Tyr343 from MtbMurE (which is substituted by Phenylalanine in MthMurE) performs a hydrogen bond with the ribose moiety while this interaction is lost in MthMurE. In addition, Phe316 still performs a π-interaction with the adenosine moiety in MthMurE although we observed a double conformation on its side chain in contrast to the Tyr343 in MtbMurE, which have a defined unique position performing a π-interaction with the ADP adenosine moiety. The hydrogen bond of the side chain of Tyr343 in MtbMurE should contribute to the stabilization of this residue in a well-defined single conformation in contrast to that observed in MthMurE. On the other hand, because of the slight displacement of the adenosine position between the two compared enzymes, Asn216 from MthMurE also loses its interaction while the same residue in MtbMurE (Asn243) is in a distance to perform a hydrogen bond with N6 of adenosine moiety of ADP (Figure 2A-B). All these differences might suport the increase of flexibility of the ADP in the binding pocket of MthMurE in contrast to MtbMurE.

The ADP binding site also has the above-mentioned $Mg^{2+}$ ions. $Mg^{2+}$-1 is in close contact with ADP and $Mg^{2+}$-2 is coordinated by His221 and further 5 water molecules (Figure 2C). $Mg^{2+}$-2 is also near Lys235 or Kcx235. This last residue has an unusual carbamylation, firstly described in *E. coli* MurE and MurD (Bertrand et al., 1999; Gordon et al., 2001), which could play a key role in the catalysis in Mur ligases, including MurD (Bertrand et al., 1999). Kcx235 performs hydrogen bonds with two water molecules (W1 and W2), which are involved in the coordination of $Mg^{2+}$-2. Although the importance of $Mg^{2+}$-2 has not been sufficiently studied, it might play, together with $Mg^{2+}$-1, an important role in positioning the catalytic residues of MurE and ATP and UAG during enzymatic catalysis (Ruane et al., 2013) (Figure 2C-D).

Comparing MthMurE with the MurE structure from *Thermotoga maritima (*TmMurE) in complex with ADP (PDB ID:4BUB), we can also observe that the residues and conformation of the ADP binding site are very conserved (Supplementary Figure 7). On the other hand, the central or nucleotide-binding domain has significant differences when the TmMurE and MthMurE structures are compared, particularly Kcx235 (Lys219 in TmMurE) and in the $Mg^{+2}$-2. Both $Mg^{+2}$-2 and the carbamylation of Lys219 are not observed in TmMurE and consequently, the interaction mode of ADP is different between

the two compared structures. Indeed, even in both MthMurE and MtbMurE, which are in different protein-ligand complexes, the diphosphate moiety of ADP performs slightly different interactions with water molecules and ligands, although most of the hydrogen bonds with protein residues are conserved (Figure 2A-D). Interestingly, in MthMurE, the ADP diphosphate moiety, despite the interaction with $Mg^{2+}$-1, also interacts through a water molecule (W3) with $Mg^{2+}$-2. On the other hand, in the MtbMurE, the unique water molecule observed in the structure (W1') (probably because of the low resolution), which should have a strong electron density, is responsible for mediating a hydrogen bond interaction between ADP diphosphate moiety to UAG. Although it is not possible to observe the water molecules that participate in the coordination of $Mg^{2+}$-2 in MtbMurE, these molecules possibly exist, and they were not modeled because of the absence of electron density caused by the low resolution of this data and consequently the binding of UAG could contribute to position the diphosphate moiety of ADP.

### 3.3. UAG Substrate binding site

The UAG substrate-binding site is located in the N-terminal domain and expands to the nucleotide-binding domain. It is possible to observe in the structure of MtbMurE that the UAG molecule makes an extensive number of hydrogen bond interactions with residues of these two domains (Figure not shown)(Basavannacharya et al., 2010b).

Since we have obtained the structure of MthMurE in the absence of UAG, we can further observe the conformational changes that may be triggered by the binding of this substrate when we compare our structure with the structure of MtbMurE:ADP:UAG ternary complex. Upon UAG binding, key conformational changes may be triggered in specific regions of both the N-terminal and the nucleotide-binding domains (Supplementary Figure 2). In our structure, as expected, the N-terminal domain has the most open conformation. Comparing the distance of the protein backbone from both structures, it is possible to observe that the loop formed by the residues 54 to 61 from MthMurE is more than 3Å away from the same region in MtbMurE (loop 80 to 87). (Figure 3A). Following this conformational change, other regions of these domains also undergo extensive movements, including the helix formed by the residues 80-86 and the loop formed by residues 22-27 (Figure 3B-C). Interestingly, in the MthMurE structure, the residues 22-34 form a long loop while in the MtbMurE structure, part of the residues that correspond

to the same regions, 28-34 in MthMurE, are structured as an α-helix. We speculate that this loop-helix transition could be caused by the binding of the substrate, and consequently, stabilize this domain in a more closed conformation upon substrate binding. However, as this region also has a low sequential identity, these conformational changes could be alternatively caused not solely by the UAG binding and so by the difference in the amino acid properties of the two enzymes (Figure 3C).

**Figure 3 – Superposition of MthMurE and MtbMurE structures showing structural differences in the UAG binding site.**

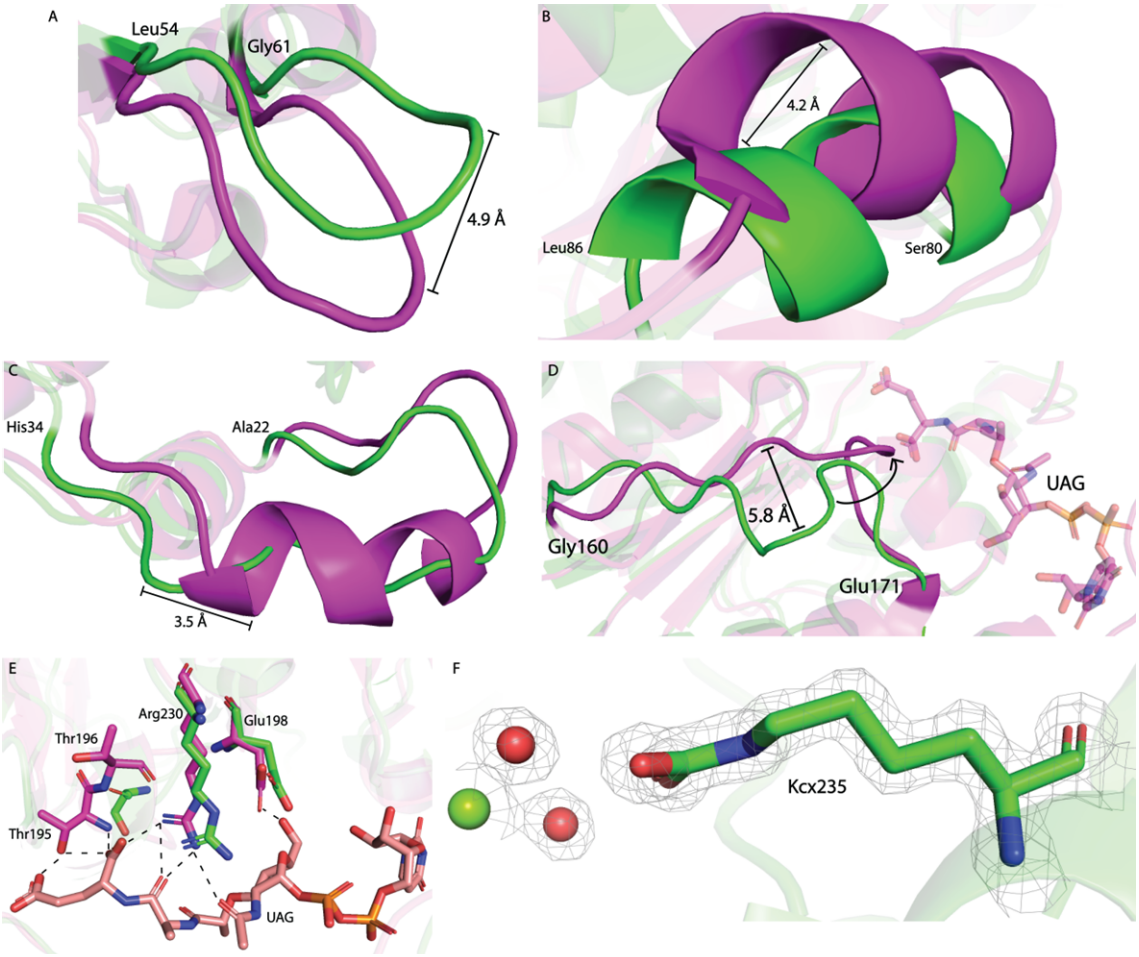


**Fig3. Superposition of MthMurE and MtbMurE structures**. The figure shows structural differences in the UAG binding site: **A** – Superposition of the MthMurE structure, in green and the MtbMurE structure in magenta, showing the differences in 54-61 loop / **B –** Superposition of the MthMurE structure and the MtbMurE structure showing the differences in 80-86 helix / **C –** Superposition of the MthMurE structure, in green and the MtbMurE structure in showing the differences in loop 22-34 / **D –** Superposition of the MthMurE structure and the MtbMurE structure

showing the differences in loop 160-171, that interacts with the peptide moiety of UAG. The proposed loop movement is shown as a black arrow. / **E –** Superposition of the MthMurE structure and the MtbMurE structure. The MtbMurE residues are shown with carbon atoms in magenta, and the MthMurE residues are shown with carbon atoms in green. UAG is shown with carbon atoms in salmon. Key residues are shown in sticks, and the interaction between the MtbMurE residues and UAG are shown as black dotted lines / **F –** Electron density contours (2Fo-Fc map) for the Kcx235 residue from MthMurE are shown in gray. The figure shows the interactions with 2 water molecules that are crucial for the $Mg^{+2}$ -2 ion coordination.

The comparison of the B-factor values between the two mycobacterial structures indicates higher flexibility of the region of the loop 22- 34 in MtbMurE while the region between residues 50-60 seems to be very flexible in both proteins (Supplementary Figure 3). Nevertheless, even with the MtbMurE structure possessing high B-factor values due to low resolution, the B-factor for the region 80-86 is higher in MthMurE, strongly suggesting that by the binding of the UAG substrate, this region adopts a more stable conformation (Supplementary Figure 3). The electron density contours are well-defined for most of the residues shown in Figure 3, which indicates that their positions should have precision even considering that these regions have a high flexibility (Supplementary Figure 4).

Since UAG also extends to the nucleotide-binding domain, it may be the cause of significant conformational changes in this region. The most significant ones are those in the loop formed by the residues 160-171 (Figure 3D), which are engaged in the active site to interact with the peptide moiety of UAG, particularly Thr195 and Thr196 in MtbMurE (or Thr168 and Thr169 in Mth). These two threonines are key catalytic residues (Basavannacharya et al., 2010a) (Figure 3E). Also upon the binding of UAG, there are some changes in the side-chain conformation of residues from the active site, particularly Glu198 (Glu171 in Mth) and Arg230 (Arg203) in MtbMurE (Figure 3E).

Kcx235 also participates in the UAG binding site contributing to the coordination of the $Mg^{2+}$-2 ion as previously mentioned (Figure 3F). This $Mg^{2+}$ should be further responsible to orientate the γ-phosphate of ATP and interact with UAG peptide moiety similarly to what is observed for *E. coli* MurD (Bertrand et al., 1999). Upon UAG binding, at least two water molecules of this region should be displaced to favor the interaction of the substrate with $Mg^{2+}$-2 during the catalysis. In comparison to MtbMurE, MthMurE has a few residue substitutions in the UAG binding site. However, these should only cause a neglectable effect on the substrate binding. These differences include the substitution of

threonines in positions 85 and 86 in MthMurE for serine and alanine, respectively, in MtbMurE (Supplementary Figure 1).

### 3.4. m-DAP binding site

Although there are several structures of MurEs in the Protein Data Bank from different organisms and different complexes with ligands, there is so far no structure with the free amino acid substrate-bound. In addition, there is only the structure of the product with the incorporation of the third amino acid, particularly L-Lysine, in the structure of MurE from *S. aureus* (Ruane et al., 2013) and, m-DAP in *E. coli* (Gordon et al., 2001). These two structures in complex with the product of the reaction allowed us to propose key insights into the specificity of the amino acid to be incorporated into the UAG between gram-positive and gram-negative bacteria (Ruane et al., 2013).

The structure of MthMurE was crystallized in the presence of m-DAP and the absence of the UAG substrate, therefore it is the first structure reported with this substrate. The analysis of our structure allowed us to obtain insights into m-DAP specificity, which is commonly incorporated in the peptidoglycan of Gram-negative and mycobacteria and into the conformational changes observed upon the binding of this molecule in the absence of UAG.

Among different MurE sequences, the residues involved in the interaction of m-DAP in gram-negative bacteria and mycobacteria are predominantly conserved and, the major difference has been attributed to the substitution of the first aspartic and the arginine from the DDNPR motif to proline and alanine (PDNPA) in gram-positive bacteria such as *S. aureus*. These substitutions alter the electrostatic charges of the binding site and consequently contribute to the specificity between L-Lys and m-DAP in gram-positive and gram-negative/actinomycetes (Ruane et al., 2013). Based on that, as expected, the m-DAP binding site is more negatively charged than the active site of *S. aureus* MurE. Thus, in MthMurE, those residues that are in contact with m-DAP include Arg398, Asp422, Asn423, Arg425, Gly476, and Glu480 (Figure 4A). In addition, we can also observe some water molecules that are indirectly involved, forming hydrogen bonds between m-DAP and the protein residues (Figure 4B).

**Figure 4 – Characterization of m-DAP binding site from MthMurE and superposition with MtbMurE showing conformational differences.**

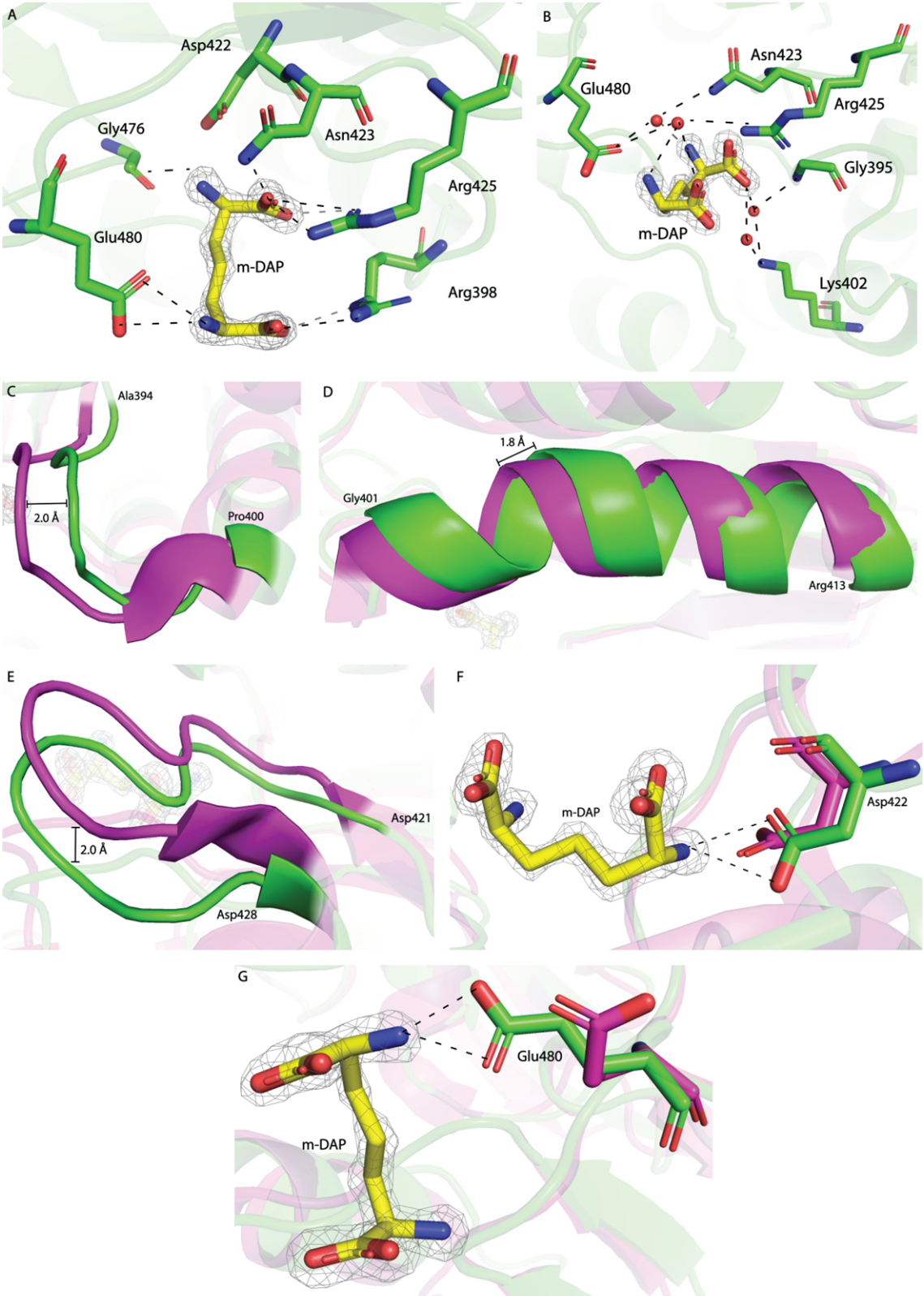

**Fig.4. m-DAP binding site in MthMurE.** Distance measuring was performed using PyMOL distance measuring tool selecting correspondent backbone residues in both proteins. **A -** Residues interacting with m-DAP from MthMurE structure, in green, m-DAP is shown in sticks with yellow carbon atoms, the electronic density contours (2Fo-Fc map) for this molecule are shown in light gray and interactions are shown as black-spotted lines. **/ B –** Hydrogen bond interaction of m-DAP and MthMurE (in green) mediated by water molecules, that are shown as red spheres. /**C -** Superposition of the MthMurE structure, in green, and MtbMurE structure, in magenta, showing the conformational differences for the 394-400 loop. The largest distance between the structures is shown as a black line / **D -** Superposition of the MthMurE structure and the MtbMurE structure, showing the differences in 401-413 helix. / **E -** Superposition of the MthMurE structure and the MtbMurE structure, showing the differences in the loop 421-428. / **F -** Superposition of the MthMurE structure, in green and the MtbMurE structure in magenta, showing the conformational changes for Asp422. / **G -** Superposition of the MthMurE structure and the MtbMurE structure, showing the conformational changes of residue Glu480.

However, there are several conformational changes in the m-DAP binding site to accommodate this substrate, particularly in the loop from the residues 394 to 400, in the α-helix formed by the residues 401 to 413 and in the loop from 421 to 427 when the structure of MthMurE is superposed to MtbMurE (Figure 4C-E). These two loop regions have key conserved residues involved in the interaction of m-DAP, including Arg398 and Asp422, Gln423 and Arg425, respectively. In addition, it is also possible to observe a conformational change in the side chain of several residues, including Asp422, which rotates in comparison to MtbMurE (Figure 4F) to optimize the hydrogen bond interaction with one of the carboxyl groups of m-DAP and Glu480 by changing its rotamer in order to interact with one of the nitrogens from the substrate (Figure 4G). Despite these conformational changes, the position of the C-terminal domain does not displace considerably (Supplementary Figure 2), and m-DAP is still far from the nucleotide-binding domain. This indicates that the binding of the UAG substrate in the presence of m-DAP should promote a conformational change in the C-terminal domain to bring together these two substrates for catalysis.

When we perform the superposition of the structure of MthMurE and EcMurE in complex with UMT, we also observe that C-terminal closes upon the nucleotide-binding site in more than 3Å. Probably the concomitant binding of UAG, ATP and m-DAP is an important requisite for the domain movements and consequently the approximation of substrates for the nucleophilic attack of the free amino acid (Supplementary figure 5).

Comparing MthMurE and EcMurE structures, we also observe that most residues that interact with m-DAP in MthMurE are conserved and they are also involved in the interaction with UMT, including Arg398 (Arg389 for EcMurE), Asp422 (Asp413 for

EcMurE), Asn423 (Asn414), Arg425 (Arg416), Gly476 (Gly464), Glu480 (Glu468). Interestingly, we can observe that m-DAP is dislocated closer to Arg398, with its carboxyl group rotated in comparison to UMT. Additionally, we also observe that could happen an expulsion of water molecules from the m-DAP binding site when the UMT product is formed. This is based on the fact, that there is only a single water molecule that is conserved between both structures and that maintains the interaction with the product UMT to residues Lys393 and Gly386 in MtbMurE. This could imply that these water molecules are necessary to maintain m-DAP in the catalytic position before UMT product formation since they also mediate interactions with residues Glu480, Arg425 and Asn423 (Figures 4B and 5B).

**Figure 5 – MthMurE and EcMurE superposition showing UMT and free m-DAP**

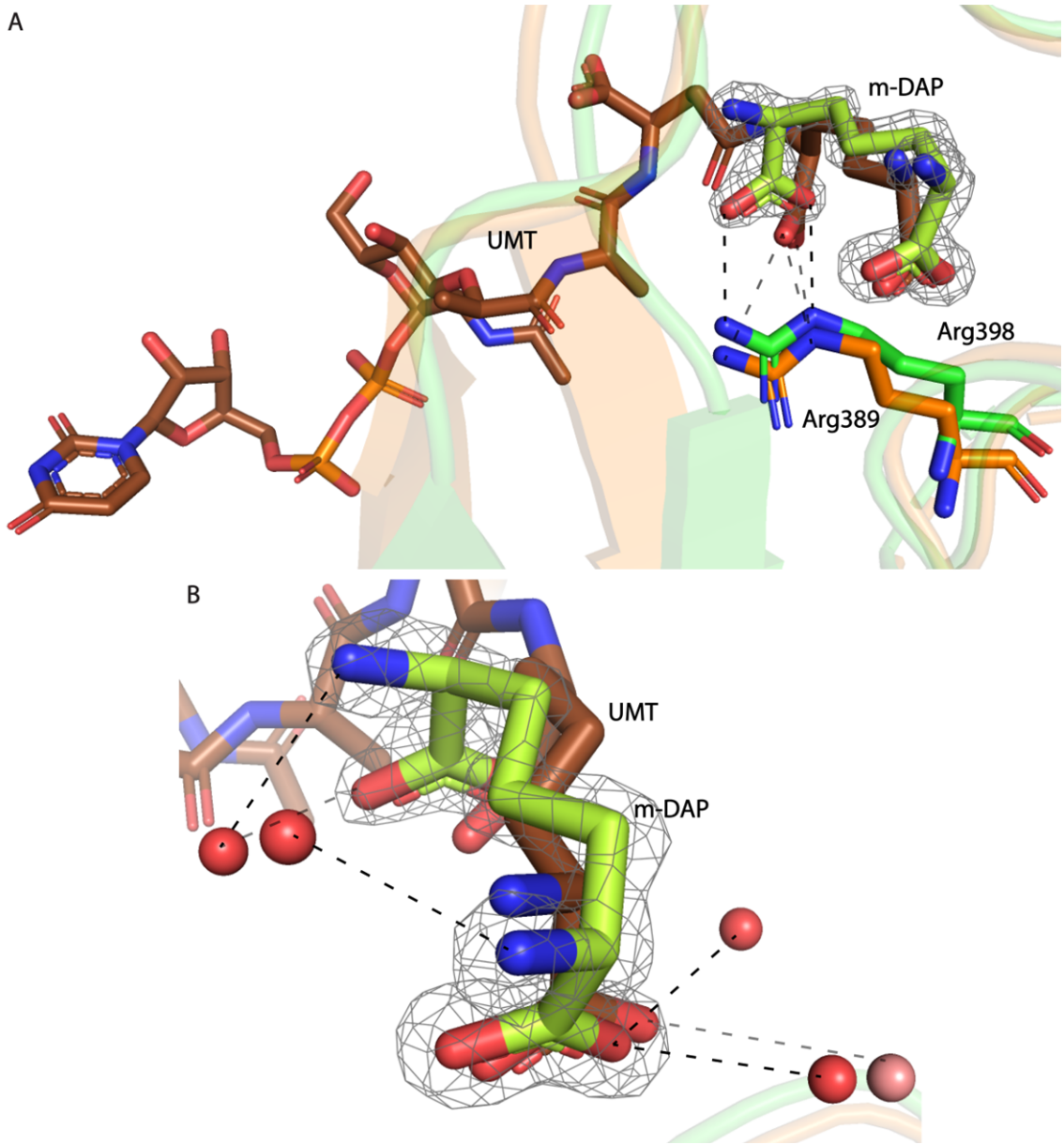

**Figure 5 – MthMurE and EcMurE superposition showing UMT and free m-DAP. A:** Superposition of MthMurE, in green, with 80% transparency and EcMurE, in orange, also with 80% transparency. Arg398 from MthMurE is shown in sticks with green carbon atoms and interactions with m-DAP are shown as black dotted lines. Arg389 from EcMurE is shown in sticks with orange carbon atoms and interactions with UMT are shown as black dotted lines / **B:** Superposition of MthMurE, in green, shown with 80% transparency and EcMurE, in orange, also shown with 80% transparency. The water molecules from MthMurE are shown as red spheres, and the water molecules from EcMurE are shown as pink spheres. UMT is shown with brown carbon atoms and m-DAP is shown with light green carbon atoms. Interactions are shown as black dotted lines PDB entry for EcMurE structure 1E8C (Gordon et al., 2001)

## 4. Insights into the motion during the catalytic cycle.

Mur ligases are known to undergo extensive conformational changes during the catalytic cycle and the ligand-free form should adopt an open conformation that should move to a closed state upon the binding of nucleotide and substrates (Smith, 2006). Based on the structural data reported so far and its comparison with the structure herein described, we can have a more complete scenario of the dynamic motions of MurE in the presence of different ligands. Thus, starting from ligand-free form (Jung et al., 2021), MurE should have the most wide-open conformation, which is also described for MurC, MurD and MurF (Basavannacharya et al., 2010a; Seo et al., 2021; Šink et al., 2016; Yan et al., 2000). In contrast, upon the binding of UAG or nucleotide, MurE should adopt a closed conformation (Gordon et al., 2001; Kouidmi et al., 2014; Smith, 2006). However, particularly in mycobacteria, based on our structure, the binding of UAG might be important to establish the bonding network necessary for the correct positioning of the nucleotide phosphates. This is based on the fact, of the weak electron density for this moiety even at 1.45Å, which could be caused by its high flexibility. Our molecular dynamics simulations also indicate that this region might have high flexibility. Although the nucleotide could bind first, based on our structural data, we propose that it would make sense that the complete engaging of the triphosphate moiety might occur after the UAG binding. However, the binding of L-Lysine or m-DAP should happen independently of the nucleotide and UAG, since this domain itself does not undergo large conformational changes. In our structure, we also observe that m-DAP triggers some conformational changes in specific regions of the C-terminal domain, but the binding of both nucleotide and UAG should be determinant for the largest conformational changes in MurE ligases.

**Summary**

Mur enzymes are essential enzymes for the biosynthesis of peptidoglycan of gram-positive, gram-negative and mycobacteria, and because of that, they are considered important targets for the development of novel antimicrobial agents. Thus, we solved the structure of MthMurE that shares a relatively high identity with MtbMurE (about 67%) at near-atomic resolution, 1.45Å, and consequently could be a good and alternative surrogate in docking and virtual screening campaigns. In addition, MthMurE structure was obtained in complex with ADP and m-DAP and the absence of UAG. This ternary complex is the first one to be described and reveals important insights into the dynamic and domain motions of the Mur ligase family.

**Acknowledgments**

We would like to thank Andrey Fabricio Ziem Nascimento from Sirius, CNPEM for the support during the X-ray data collection. This project is funded by FAPESP grant number 2020/03850-9. Marcio thanks to CNPq for the fellowship 208998/2020-0 and Nicolas and Catharina received a fellowship from FAPESP, numbers 2019/17037-0 and 2016/18721-4, respectively.

**References**

Abraham, M.J., Murtola, T., Schulz, R., Páll, S., Smith, J.C., Hess, B., Lindah, E., 2015. Gromacs: High performance molecular simulations through multi-level parallelism from laptops to supercomputers. SoftwareX 1–2, 19–25. https://doi.org/10.1016/j.softx.2015.06.001

Adams, P.D., Afonine, P. V., Bunkóczi, G., Chen, V.B., Echols, N., Headd, J.J., Hung, L.W., Jain, S., Kapral, G.J., Grosse Kunstleve, R.W., McCoy, A.J., Moriarty, N.W., Oeffner, R.D., Read, R.J., Richardson, D.C., Richardson, J.S., Terwilliger, T.C., Zwart, P.H., 2011. The Phenix software for automated determination of macromolecular structures. Methods 55, 94–106. https://doi.org/10.1016/J.YMETH.2011.07.005

Alderwick, L.J., Harrison, J., Lloyd, G.S., Birch, H.L., 2015. The Mycobacterial Cell Wall—Peptidoglycan and Arabinogalactan. Cold Spring Harb. Perspect. Med. 5,

1–16. https://doi.org/10.1101/CSHPERSPECT.A021113

Aliashkevich, A., Cava, F., 2021. LD-transpeptidases: the great unknown among the peptidoglycan cross-linkers. FEBS J. https://doi.org/10.1111/FEBS.16066

Barreteau, H., Kovač, A., Boniface, A., Sova, M., Gobec, S., Blanot, D., 2008. Cytoplasmic steps of peptidoglycan biosynthesis. FEMS Microbiol. Rev. 32, 168–207. https://doi.org/10.1111/J.1574-6976.2008.00104.X

Basavannacharya, C., Moody, P.R., Munshi, T., Cronin, N., Keep, N.H., Bhakta, S., 2010a. Essential residues for the enzyme activity of ATP-dependent MurE ligase from Mycobacterium tuberculosis. Protein Cell 1, 1011. https://doi.org/10.1007/S13238-010-0132-9

Basavannacharya, C., Robertson, G., Munshi, T., Keep, N.H., Bhakta, S., 2010b. ATP-dependent MurE ligase in Mycobacterium tuberculosis: biochemical and structural characterisation. Tuberculosis (Edinb). 90, 16–24. https://doi.org/10.1016/J.TUBE.2009.10.007

Batson, S., De Chiara, C., Majce, V., Lloyd, A.J., Gobec, S., Rea, D., Fülöp, V., Thoroughgood, C.W., Simmons, K.J., Dowson, C.G., Fishwick, C.W.G., De Carvalho, L.P.S., Roper, D.I., 2017. Inhibition of D-Ala:D-Ala ligase through a phosphorylated form of the antibiotic D-cycloserine. Nat. Commun. 8. https://doi.org/10.1038/S41467-017-02118-7

Bertrand, J.A., Auger, G., Fanchon, E., Martin, L., Blanot, D., Van Heijenoort, J., Dideberg, O., 1997. Crystal structure of UDP-N-acetylmuramoyl-L-alanine:D-glutamate ligase from Escherichia coli. EMBO J. 16, 3416–3425. https://doi.org/10.1093/EMBOJ/16.12.3416

Bertrand, J.A., Auger, G., Martin, L., Fanchon, E., Blanot, D., Le Beller, D., Van Heijenoort, J., Dideberg, O., 1999. Determination of the MurD mechanism through crystallographic analysis of enzyme complexes. J. Mol. Biol. 289, 579–590. https://doi.org/10.1006/JMBI.1999.2800

Cochrane, S.A., Lohans, C.T., 2020. Breaking down the cell wall: Strategies for antibiotic discovery targeting bacterial transpeptidases. Eur. J. Med. Chem. 194, 112262. https://doi.org/10.1016/J.EJMECH.2020.112262

Davis, I.W., Leaver-Fay, A., Chen, V.B., Block, J.N., Kapral, G.J., Wang, X., Murray, L.W., Arendall, W.B., Snoeyink, J., Richardson, J.S., Richardson, D.C., 2007. MolProbity: all-atom contacts and structure validation for proteins and nucleic acids. Nucleic Acids Res. 35, W375–W383. https://doi.org/10.1093/NAR/GKM216

Dean, A.S., Tosas Auguet, O., Glaziou, P., Zignol, M., Ismail, N., Kasaeva, T., Floyd, K., 2022. 25 years of surveillance of drug-resistant tuberculosis: achievements, challenges, and way forward. Lancet. Infect. Dis. https://doi.org/10.1016/S1473-3099(21)00808-2

Duncan, K., van Heijenoort, J., Walsh, C.T., 1990. Purification and characterization of the D-alanyl-D-alanine-adding enzyme from Escherichia coli. Biochemistry 29, 2379–2386. https://doi.org/10.1021/BI00461A023

Egan, A.J.F., Biboy, J., van't Veer, I., Breukink, E., Vollmer, W., 2015. Activities and regulation of peptidoglycan synthases. Philos. Trans. R. Soc. Lond. B. Biol. Sci. 370. https://doi.org/10.1098/RSTB.2015.0031

Egan, A.J.F., Errington, J., Vollmer, W., 2020. Regulation of peptidoglycan synthesis and remodelling. Nat. Rev. Microbiol. 2020 188 18, 446–460. https://doi.org/10.1038/s41579-020-0366-3

Emsley, P., Lohkamp, B., Scott, W.G., Cowtan, K., 2010. Features and development of Coot. Acta Crystallogr. D. Biol. Crystallogr. 66, 486–501. https://doi.org/10.1107/S0907444910007493

Evans, P.R., Murshudov, G.N., 2013. How good are my data and what is the resolution? urn:issn:0907-4449 69, 1204–1214. https://doi.org/10.1107/S0907444913000061

Falk, P.J., Ervin, K.M., Volk, K.S., Ho, H.T., 1996. Biochemical evidence for the formation of a covalent acyl-phosphate linkage between UDP-N-acetylmuramate and ATP in the Escherichia coli UDP-N-acetylmuramate:L-alanine ligase-catalyzed reaction. Biochemistry 35, 1417–1422. https://doi.org/10.1021/BI952078B

Favini-Stabile, S., Contreras-Martel, C., Thielens, N., Dessen, A., 2013. MreB and MurG as scaffolds for the cytoplasmic steps of peptidoglycan biosynthesis.

Environ. Microbiol. 15, 3218–3228. https://doi.org/10.1111/1462-2920.12171/SUPPINFO

Gordon, E., Flouret, B., Chantalat, L., Van Heijenoort, J., Mengin-Lecreulx, D., Dideberg, O., 2001. Crystal Structure of UDP-N-acetylmuramoyl-l-alanyl-d-glutamate:meso-Diaminopimelate Ligase from Escherichia Coli. J. Biol. Chem. 276, 10999–11006. https://doi.org/10.1074/JBC.M009835200

Guzman, J.D., Pesnot, T., Barrera, D.A., Davies, H.M., McMahon, E., Evangelopoulos, D., Mortazavi, P.N., Munshi, T., Maitra, A., Lamming, E.D., Angell, R., Gershater, M.C., Redmond, J.M., Needham, D., Ward, J.M., Cuca, L.E., Hailes, H.C., Bhakta, S., 2015. Tetrahydroisoquinolines affect the whole-cell phenotype of Mycobacterium tuberculosis by inhibiting the ATP-dependent MurE ligase. J. Antimicrob. Chemother. 70, 1691–1703. https://doi.org/10.1093/JAC/DKV010

Hervin, V., Arora, R., Rani, J., Ramchandran, S., Bajpai, U., Agrofoglio, L.A., Roy, V., 2020. Design and Synthesis of Various 5'-Deoxy-5'-(4-Substituted-1,2,3-Triazol-1-yl)-Uridine Analogues as Inhibitors of Mycobacterium tuberculosis Mur Ligases. Molecules 25. https://doi.org/10.3390/MOLECULES25214953

Hrast, M., Sosič, I., Šink, R., Gobec, S., 2014. Inhibitors of the peptidoglycan biosynthesis enzymes MurA-F. Bioorg. Chem. 55, 2–15. https://doi.org/10.1016/J.BIOORG.2014.03.008

Jung, K.H., Kim, Y.G., Kim, C.M., Ha, H.J., Lee, C.S., Lee, J.H., Park, H.H., 2021. Wide-open conformation of UDP-MurNc-tripeptide ligase revealed by the substrate-free structure of MurE from Acinetobacter baumannii. FEBS Lett. 595, 275–283. https://doi.org/10.1002/1873-3468.14007

Kabsch, W., 2010. XDS. Acta Crystallogr. Sect. D Biol. Crystallogr. 66, 125. https://doi.org/10.1107/S0907444909047337

Kouidmi, I., Levesque, R.C., Paradis-Bleau, C., 2014. The biology of Mur ligases as an antibacterial target. Mol. Microbiol. 94, 242–253. https://doi.org/10.1111/MMI.12758

Lawrence, C.M., Ray, S., Babyonyshev, M., Galluser, R., Borhani, D.W., Harrison, S.C., 1999. Crystal structure of the ectodomain of human transferrin receptor.

Science 286, 779–782. https://doi.org/10.1126/SCIENCE.286.5440.779

Libreros-Zúniga, G.A., Dos Santos Silva, C., Salgado Ferreira, R., Dias, M.V.B., 2019. Structural Basis for the Interaction and Processing of β-Lactam Antibiotics by l, d - Transpeptidase 3 (Ldt Mt3 ) from Mycobacterium tuberculosis. ACS Infect. Dis. 5, 260–271. https://doi.org/10.1021/acsinfecdis.8b00244

Liebschner, D., Afonine, P. V., Baker, M.L., Bunkoczi, G., Chen, V.B., Croll, T.I., Hintze, B., Hung, L.W., Jain, S., McCoy, A.J., Moriarty, N.W., Oeffner, R.D., Poon, B.K., Prisant, M.G., Read, R.J., Richardson, J.S., Richardson, D.C., Sammito, M.D., Sobolev, O. V., Stockwell, D.H., Terwilliger, T.C., Urzhumtsev, A.G., Videau, L.L., Williams, C.J., Adams, P.D., 2019. Macromolecular structure determination using X-rays, neutrons and electrons: Recent developments in Phenix. Acta Crystallogr. Sect. D Struct. Biol. 75, 861–877. https://doi.org/10.1107/S2059798319011471

Madura, J.D., Jorgensen, W.L., Chandrasekhar, J., Impey, R.W., Klein, M.L., 1983. Comparison of simple potential functions for simulating liquid water. aip.scitation.org 79, 926. https://doi.org/10.1063/1.445869

Marquardt, J.L., Brown, E.D., Walsh, C.T., Lane, W.S., Haley, T.M., Ichikawa, Y., Wong, C.H., 1994. Kinetics, stoichiometry, and identification of the reactive thiolate in the inactivation of UDP-GlcNAc enolpyruvoyl transferase by the antibiotic fosfomycin. Biochemistry 33, 10646–10651. https://doi.org/10.1021/BI00201A011

Mengin-Lecreulx, D., Falla, T., Didier Blanot, †, Van Heijenoort, J., Adams, D.J., Chopra, I., 1999. Expression of the Staphylococcus aureus UDP-N-Acetylmuramoyl-L-Alanyl-D-Glutamate:L-Lysine Ligase in Escherichia coli and Effects on Peptidoglycan Biosynthesis and Cell Growth. J. Bacteriol. 181, 5909–5914.

Ruane, K.M., Lloyd, A.J., Fülöp, V., Dowson, C.G., Barreteau, H., Boniface, A., Dementin, S., Blanot, D., Mengin-Lecreulx, D., Gobec, S., Dessen, A., Roper, D.I., 2013. Specificity determinants for lysine incorporation in Staphylococcus aureus peptidoglycan as revealed by the structure of a MurE enzyme ternary complex. J. Biol. Chem. 288, 33439–33448. https://doi.org/10.1074/JBC.M113.508135

Ruiz, N., 2016. Lipid Flippases for Bacterial Peptidoglycan Biosynthesis. Lipid Insights 8, 21–31. https://doi.org/10.4137/LPI.S31783

Schrödinger, LLC, 2015. The {PyMOL} Molecular Graphics System, Version~1.8.

Seo, P.W., Park, S.Y., Hofmann, A., Kim, J.S., 2021. Crystal structures of UDP-N-acetylmuramic acid L-alanine ligase (MurC) from Mycobacterium bovis with and without UDP-N-acetylglucosamine. Acta Crystallogr. Sect. D, Struct. Biol. 77, 618–627. https://doi.org/10.1107/S2059798321002199

Shaku, M., Ealand, C., Matlhabe, O., Lala, R., Kana, B.D., 2020. Peptidoglycan biosynthesis and remodeling revisited. Adv. Appl. Microbiol. 112, 67–103. https://doi.org/10.1016/BS.AAMBS.2020.04.001

Shinde, Y., Ahmad, I., Surana, S., Patel, H., 2021. The Mur Enzymes Chink in the Armour of Mycobacterium tuberculosis cell wall. Eur. J. Med. Chem. 222. https://doi.org/10.1016/J.EJMECH.2021.113568

Šink, R., Kotnik, M., Zega, A., Barreteau, H., Gobec, S., Blanot, D., Dessen, A., Contreras-Martel, C., 2016. Crystallographic Study of Peptidoglycan Biosynthesis Enzyme MurD: Domain Movement Revisited. PLoS One 11. https://doi.org/10.1371/JOURNAL.PONE.0152075

Smith, C.A., 2006. Structure, function and dynamics in the mur family of bacterial cell wall ligases. J. Mol. Biol. 362, 640–655. https://doi.org/10.1016/J.JMB.2006.07.066

Soteras Gutiérrez, I., Lin, F.Y., Vanommeslaeghe, K., Lemkul, J.A., Armacost, K.A., Brooks, C.L., MacKerell, A.D., 2016. Parametrization of halogen bonds in the CHARMM general force field: Improved treatment of ligand–protein interactions. Bioorg. Med. Chem. 24, 4812–4825. https://doi.org/10.1016/J.BMC.2016.06.034

Straume, D., Piechowiak, K.W., Kjos, M., Håvarstein, L.S., 2021. Class A PBPs: It is time to rethink traditional paradigms. Mol. Microbiol. 116, 41–52. https://doi.org/10.1111/MMI.14714

Vagin, A., Teplyakov, A., 2010. Molecular replacement with MOLREP. Acta Crystallogr. D. Biol. Crystallogr. 66, 22–25.

https://doi.org/10.1107/S0907444909042589

Vollmer, W., Blanot, D., De Pedro, M.A., 2008. Peptidoglycan structure and architecture. FEMS Microbiol. Rev. 32, 149–167. https://doi.org/10.1111/J.1574-6976.2007.00094.X

Walker, J.E., Saraste, M., Runswick, M.J., Gay, N.J., 1982. Distantly related sequences in the alpha- and beta-subunits of ATP synthase, myosin, kinases and other ATP-requiring enzymes and a common nucleotide binding fold. EMBO J. 1, 945–951. https://doi.org/10.1002/J.1460-2075.1982.TB01276.X

World Health Organization, 2021. Global Tuberculosis Report 2021, Global Tuberculosis Report.

Yan, Y., Munshi, S., Leiting, B., Anderson, M.S., Chrzas, J., Chen, Z., 2000. Crystal structure of Escherichia coli UDPMurNAc-tripeptide d-alanyl-d-alanine-adding enzyme (MurF) at 2.3 A resolution. J. Mol. Biol. 304, 435–445. https://doi.org/10.1006/JMBI.2000.4215

Zaveri, K., Kiranmayi, P., 2016. Screening of Potential Lead Molecule as Novel MurE Inhibitor: Virtual Screening, Molecular Dynamics and In Vitro Studies. Curr. Comput. Aided-Drug Des. 13, 8–21. https://doi.org/10.2174/1573409912666161010142943

Zoeiby, E., Sanschagrin, F, Levesque, R C, El Zoeiby, A., Sanschagrin, François, Levesque, Roger C, 2003. Structure and function of the Mur enzymes: development of novel inhibitors. Mol. Microbiol. 47, 1–12. https://doi.org/10.1046/J.1365-2958.2003.03289.X